

Scheduling for TWDM-EPON-Based Fronthaul Without a Dedicated Registration Wavelength

Akash Kumar, Sourav Dutta, and Goutam Das,

Abstract—The adoption of Centralized Radio Access Network (C-RAN) architectures requires fronthaul systems capable of carrying large volumes of radio data while meeting stringent delay and jitter requirements. Ethernet Passive Optical Networks (EPONs) have emerged as a promising fronthaul solution due to their cost efficiency and compatibility with existing infrastructure. However, the traditional registration process for EPON systems halts the ongoing data transmissions during the registration period, thereby violating the enhanced Common Public Radio Interface (eCPRI) delay and jitter requirements. This limitation has been acknowledged by the ITU-T, which recommends the use of a dedicated wavelength channel for registration, leading to inefficient bandwidth utilization. In this paper, we propose a novel scheduling framework for a Time and Wavelength Division Multiplexed (TWDM) EPON-based fronthaul that enables periodic registration without wasting an additional wavelength channel. Performance evaluation demonstrates that the proposed method achieves up to a 71% increase in the number of Radio Units (RUs) supported for a given number of wavelength channels, compared to a baseline scheme employing a dedicated registration wavelength.

Index Terms—C-RAN, Fronthaul, Lower-Layer Split, EPON, TWDM, Registration

I. INTRODUCTION

Emerging applications such as Multi-Sensory Extended Reality (XR), autonomous vehicle communication, and cooperative transmission for users near coverage boundaries rely on tight coordination among neighboring cells to maintain consistent coverage quality [1]. However, in conventional Distributed Radio Access Network (D-RAN) architectures, both radio transmission and baseband processing are co-located at individual cell sites, forcing each base station to operate with only a limited, localized view of the network [2], [3]. To overcome this limitation, the Centralized Radio Access Network (C-RAN) architecture decouples baseband processing from remote radio transmission and moves it in shared processing pools [4]. This architecture enables advanced inter-cell coordination techniques such as joint scheduling and dynamic resource allocation across multiple cells, supports computational resource pooling and virtualization, and facilitates simpler network upgrades.

In the Next Generation Radio Access Network (NG-RAN) architecture defined by 3GPP in TS 38.401 [5], the access network is composed of Central Units (CUs), Distributed Units (DUs), and Radio Units (RUs), organized hierarchically, as illustrated in Fig. 1. Within this architecture, baseband

A. Kumar and G. Das are with the Department of Electronics and Electrical Communication Engineering, Indian Institute of Technology Kharagpur, India.

S. Dutta is with the School of Computing and Electrical Engineering, Indian Institute of Technology Mandi, India.

processing is partitioned through functional splits, with higher-layer splits (HLS) defining the functional separation between the CU and DU, and lower-layer splits (LLS) defining the functional separation between the DU and RU [5].

Among the lower-layer split (LLS) options, the Split 7.x family (i.e., Splits 7.1, 7.2, and 7.3) and Split 8 are of particular interest in this work. Splits 7.1, 7.2, and 7.3 correspond to intra-PHY functional splits, in which lower physical-layer processing is partitioned between the DU and RU, whereas Split 8 centralizes the entire physical layer at the DU, leaving the RU responsible only for radio-frequency processing and radio transmission and reception [6]. Consequently, the DU–RU interface, referred to as the fronthaul, carries partially processed frequency-domain data in the case of the Split 7.x family and digitized time-domain radio samples in the case of Split 8. These splits impose the most stringent fronthaul requirements, including extremely high bandwidth demands, sub-millisecond one-way delay budgets, and jitter tolerances on the order of tens of nanoseconds [6], [7].

To meet the extreme bandwidth and stringent latency requirements imposed by LLS options, optical transport technologies are generally preferred, as wireless fronthaul solutions are fundamentally constrained by limited spectrum availability, interference, and capacity [8]. Among optical access solutions, Ethernet Passive Optical Networks (EPONs) have attracted significant interest due to their mature ecosystem, cost efficiency, and compatibility with existing deployed fiber infrastructure. Fronthaul traffic is typically transported using the Common Public Radio Interface (CPRI) [9] or its packet-based evolution, the enhanced CPRI (eCPRI) protocol [10].

Practical EPON fronthaul deployments require a registration mechanism, since the set of RUs carrying traffic may vary over time due to changes in traffic demand or because RUs may be powered on or off, newly added, replaced, or temporarily taken out of service. Registration enables the fronthaul to discover active RUs, perform upstream ranging for timing alignment, and include them in upstream scheduling, while deregistration ensures that inactive RUs are excluded from transmission.

To enable registration, the traditional EPON standard IEEE 802.3av [11] inserts periodic registration windows of fixed size where ongoing transmissions are halted and the channel is used exclusively for the registration process. These windows must be at least as large as the round-trip time (RTT) required for ONU discovery, and such long pauses inevitably violate the fronthaul delay restrictions. This issue is examined in detail in Section III.

The ITU-T acknowledged this problem and proposed dedicating a wavelength channel exclusively to the registration process, while carrying out regular transmissions over the

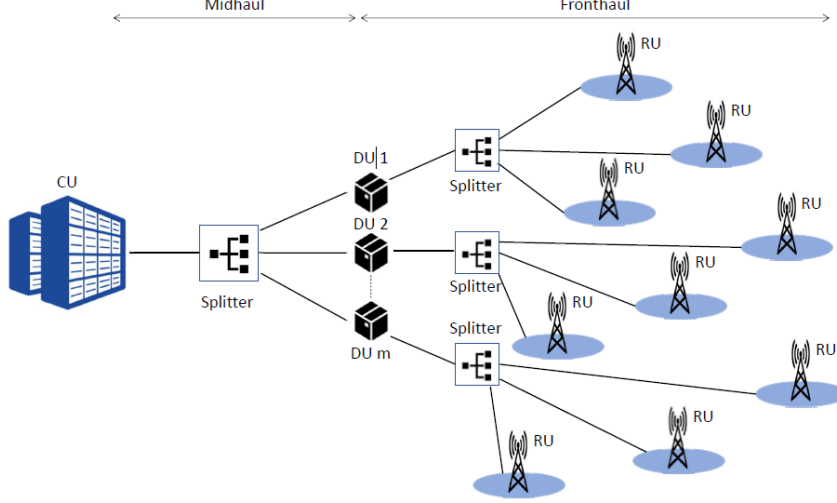


Fig. 1. X-haul Architecture (to be edited)

remaining wavelength channels [12]. While this approach avoids delay and jitter violations caused by the registration process, it ends up wasting an entire wavelength channel on a process that requires very little bandwidth.

In this paper, we propose a scheduling framework for a Time and Wavelength Division Multiplexed (TWDM) EPON-based fronthaul architecture that eliminates the need to dedicate a wavelength channel for registration. Instead, we insert periodic registration windows by dynamically selecting a wavelength when registration is required and temporarily redistributing all ONUs across the remaining wavelengths. This strategy ensures that registration can proceed on one wavelength while uninterrupted fronthaul traffic continues on the others, thereby meeting latency requirements for all RUs without compromising spectral efficiency.

However, during such registration periods, the reduced available bandwidth causes eCPRI traffic to accumulate at the ONU buffers, introducing additional delay for eCPRI frames, which must be carefully controlled to satisfy the strict delay budget. To address this, we formulated a delay-bounded optimization problem that maximizes the number of supported RUs for a given number of wavelength channels.

The remainder of this paper is organized as follows. Section II reviews prior work related to fronthaul scheduling and ONU registration. Section III presents the motivation for this study and discusses the required background. Section IV describes the system model and the proposed scheduling framework. Section V presents the optimization formulation and associated constraints. Section VI reports the performance evaluation under varying system parameters. Section VII concludes the paper.

II. RELATED WORKS

Beyond the ITU-T approach of dedicating a wavelength exclusively for registration, prior work on EPON-based fronthaul can be broadly divided into two directions. One line of research primarily focuses on scheduling and wavelength

management, where the registration process is not a central design focus. Another line of research explicitly addresses the registration process itself, proposing ways to eliminate the registration window or reduce its impact.

In the scheduling-focused direction, Liang et al. [13] proposed a distributed wavelength selection mechanism for C-RAN fronthaul in which ONUs autonomously form virtual TDM-PONs. Although the protocol includes a Multipoint Control Protocol (MPCP) quiet window to support ONU registration, this operation is treated as a basic control exchange and retains the minimum requirement of an RTT-sized registration window. The work does not consider how such windows can be accommodated without interrupting ongoing eCPRI traffic, which violates the delay and jitter constraints expected in mobile fronthaul systems.

Similar scheduling-centric formulations that abstract away the registration process have also been explored in [14], where a TDM-based uplink scheduling framework is proposed for heterogeneous fronthaul traffic without explicitly addressing ONU registration.

Addressing the registration process itself, hitless activation techniques embed ranging or discovery signals within ongoing transmissions to eliminate the need for registration windows entirely [15], [16]. While these physical-layer approaches demonstrate that interruption-free registration is theoretically possible, they rely on non-standard signal processing and modified optical transceivers, making them incompatible with the existing, widely deployed EPON hardware ecosystem and impractical for near-term fronthaul deployment.

Adaptive registration schemes dynamically resize the discovery window duration based on network conditions, as studied for TDM-PON in [17] and TWDM-PON with ONU migrations in [18]. However, these schemes still fundamentally rely on explicit quiet windows of at least one RTT to guarantee correct ranging, and were not designed for mobile fronthaul with sub-millisecond timing constraints.

Overall, prior solutions either shrink the registration window

without eliminating the fundamental need for it, or require sophisticated hardware that is not currently commercially viable. To the best of our knowledge, no existing method enables registration on arbitrary wavelengths while maintaining continuous multi-wavelength fronthaul traffic. This gap motivates the framework proposed in this paper.

III. MOTIVATION AND BACKGROUND

In this work, we propose an scheduling framework for a fronthaul system implemented over an Ethernet Passive Optical Network (EPON), where a centralized Optical Line Terminal (OLT) interfaces with the DU and is responsible for aggregating traffic from multiple Optical Network Units (ONUs) located at remote sites, each servicing a distinct RU. The fronthaul traffic is transported using the eCPRI protocol, which requires high bandwidth and imposes stringent delay and jitter constraints.

In conventional EPON systems, the registration process follows the IEEE 802.3av [11] specification, which defines how newly added or previously inactive ONUs request network access. The channel is effectively divided into two distinct phases: a **transmission window** and a **registration window** (refer Fig. 2). During the transmission window, all registered ONUs send user data according to the grant schedule assigned by the OLT. Periodically, the OLT schedules a registration window, a specific interval during which normal transmissions are halted (creating a “quiet period”) to allow unregistered ONUs to initiate the access procedure.

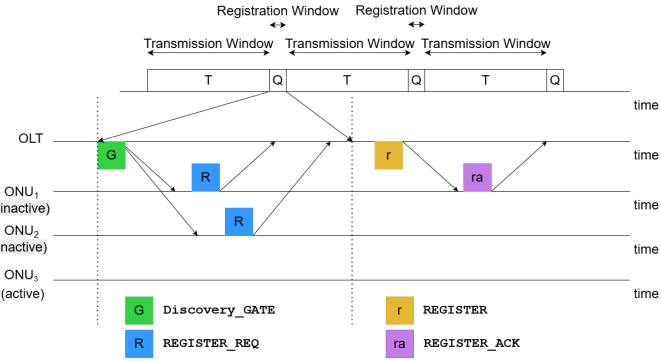


Fig. 2. Standard EPON registration process.

The standard registration process entails a four-step message exchange, although only the initial contention phase relies on the dedicated registration window. The OLT begins by broadcasting a `Discovery_GATE` message to define the start of a registration window of known duration. Any unregistered ONU seeking to join the network then randomly selects a transmission instant within this window and sends a `REGISTER_REQ` message.

Since these requests are contention-based, multiple ONUs may transmit simultaneously, resulting in collisions. In the event of a collision, an ONU defers its registration attempt using a randomized back-off and retries in a subsequent registration window.

Upon successfully receiving a request, the OLT assigns a Logical Link Identifier (LLID) to the ONU and replies with a

unicast `REGISTER` message carrying the necessary configuration parameters. The ONU then completes the handshake by transmitting a `REGISTER_ACK` message, after which it can participate in subsequent grant cycles. Note that the latter two messages are not constrained by the registration window and are transmitted during normal operation.

To ensure that the entire registration exchange fits within the available window, the window duration must exceed the maximum Round-Trip Time (RTT) of the network. With fiber distances of up to 20 km, the maximum RTT is roughly 200 μ s. To provide sufficient margin for random back-off and processing delays, the registration window T_{reg} is typically set slightly higher, around 250 μ s. As registration requires bidirectional control message exchange, a quiet window must be enforced in both the upstream and downstream channels.

However, halting transmissions for the duration of the registration window increases the waiting time for the frames in the next scheduled slot. As illustrated in Fig. 3, if traffic is paused for a period T_{reg} , then frames transmitted in the next slot after the registration window experience a scheduling delay of $(T_{\text{reg}} + T_C)$, where T_C denotes the interval between two successive transmission slots allocated to the same ONU. Therefore, the scheduling delay budget D_b must satisfy

$$D_b \geq T_{\text{reg}} + T_C. \quad (1)$$

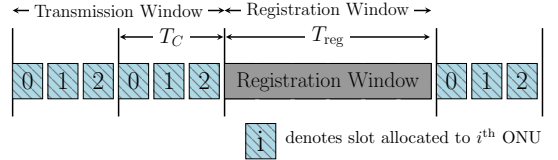


Fig. 3. Standard EPON scheduling illustrating the periodic interruption of the transmission window by the mandatory registration window.

In eCPRI-based fronthaul systems, the one-way delay budget is only 250 μ s [7]. After accounting for a propagation delay of roughly 100 μ s, the remaining scheduling budget is approximately 150 μ s. As a result, halting transmissions for a registration window of 250 μ s inevitably violates this constraint. Therefore, the standard EPON registration procedure cannot be directly applied in fronthaul deployments.

The ITU-T Recommendation G.9804.2 [12] addresses this registration-induced delay violations by dedicating a wavelength exclusively to the registration process, thereby satisfying eCPRI delay and jitter requirements, but at the cost of reduced spectral efficiency. In the next section, we explain how our approach addresses these issues.

IV. PROPOSED FRAMEWORK

We consider a TWDM-EPON fronthaul system in which each RU exchanges eCPRI traffic with the DU at a configured eCPRI line rate R_C , although the instantaneous transmitted rate may be lower depending on the user traffic. This rate is assumed to be identical for all RUs so that we can focus on the core scheduling mechanism for clearer analytical exposition. Extensions to heterogeneous scenarios, where different RUs operate at different eCPRI rates, can be handled by the

same framework by appropriately distributing unequal traffic loads across wavelengths to maintain balanced utilization. The remainder of the formulation remains unchanged.

For the remainder of the paper, we focus on the upstream direction only, noting that the same modeling and scheduling principles apply to the downstream direction as well. Here, the fronthaul system employs W wavelength channels, each operating at a line rate of R_E bits per second. Each wavelength channel is shared among N ONUs when the registration process is not being carried out. We denote each ONU as $\mathcal{N}(\lambda, i_n)$, where $\lambda \in \{0, 1, \dots, W-1\}$ denotes the wavelength index, and $i_n \in \{0, 1, \dots, N-1\}$ denotes its slot index in a cycle outside registration periods. This indexing is purely logical and does not imply permanent physical binding of an ONU to a specific wavelength or slot.

Accordingly, we assume that ONUs are equipped with tunable optical transceivers (or multiple fixed lasers), allowing them to switch between wavelength channels across cycles as required by the proposed redistribution. Such tunable ONUs are already supported in TWDM-EPON standards and commercial implementations, making this assumption practical. In typical operation, ONUs remain on their assigned wavelengths during non-registration cycles and only retune during registration-related events; even when retuning is required, at least one full scheduling cycle is available for wavelength switching.

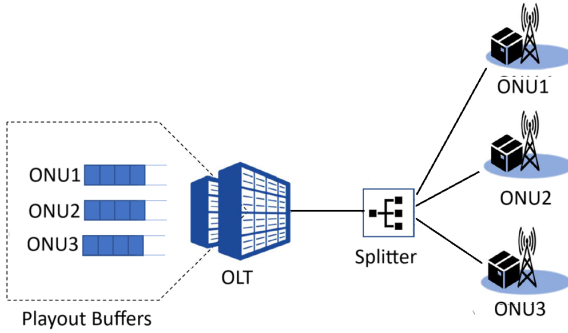


Fig. 4. Employing playout buffers to meet the eCPRI jitter requirement.

Since multiple ONUs share each wavelength channel, an ONU transmits only during its assigned time slot, resulting in a periodic but non-continuous transmission pattern. In contrast, eCPRI traffic requires a continuous stream of packets at the receiver, with a stringent jitter constraint of less than 65 ns [5]. To address this, playout buffers are employed at the DU (see Fig. 4) to temporarily store incoming data and smooth the bursty arrivals into a uniform output stream, thereby meeting the jitter requirement. The sizes of the transmission slots and the playout buffers must be jointly designed to avoid both buffer underflow and overflow.

To enable the registration process, we place periodic registration windows on an arbitrary wavelength, while temporarily redistributing all the ONUs across the remaining $(W-1)$ wavelength channels during that interval, as shown in Fig. 5. As bandwidth available for transmission is reduced in these cycles (referred to as Registration cycles here), extra data accu-

mulates in the ONU buffers. In the cycles apart from the ones used for registration (referred to as Non-registration cycles here), all the available wavelengths are used for transmission, and the extra data accumulated during the registration cycles is cleared from the ONU buffers.

Specifically, the allocation follows a round-robin, row-wise order: we first assign the first slot on each wavelength to $\mathcal{N}(0, 0), \mathcal{N}(1, 0), \dots, \mathcal{N}(W-2, 0)$, then the next set of slots to $\mathcal{N}(W-1, 0), \mathcal{N}(0, 1), \dots, \mathcal{N}(W-3, 1)$, and so on, continuing until all $\mathcal{N}(W-1, N-1)$ are reassigned (see Figs. 5 and 6).

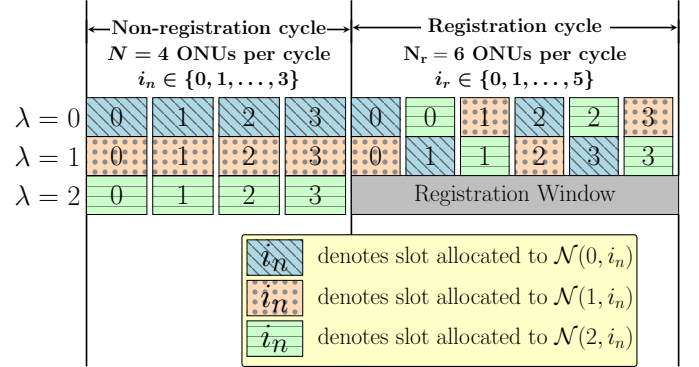


Fig. 5. Example of ONU redistribution for $N = 4$ and $W = 3$. Here, $N_r = 6$ (from Eq. 2), and the slot index i_r is computed using Eq. 3.

To maintain support for all the ONUs during registration cycles, the remaining $(W-1)$ wavelengths must collectively support the total $N \cdot W$ ONUs. As a result, each of these wavelengths supports up to

$$N_r = \left\lceil \frac{N \cdot W}{W-1} \right\rceil \quad (2)$$

ONUs during registration cycles.

Note that if N is not an exact factor of $(W-1)$, some wavelengths will need to accommodate only (N_r-1) ONUs, whereas the remaining wavelengths will continue to support N_r ONUs each (see Fig. 6). Since registration cycles occur over a much smaller duration (on the order of a few hundred microseconds) compared to non-registration data cycles (on the order of a few hundred milliseconds), the presence of these vacant slots does not result in any significant throughput degradation.

Under this redistribution, the slot index assigned to ONU $\mathcal{N}(\lambda, i_n)$ during a registration cycle is given by

$$i_r = \left\lfloor \frac{W i_n + \lambda}{W-1} \right\rfloor. \quad (3)$$

where $i_r \in \{0, 1, \dots, N_r-1\}$. The floor operation reflects the row-wise, round-robin assignment across the remaining $(W-1)$ wavelengths, mapping consecutive ONUs to successive slots until all $N \cdot W$ ONUs are accommodated.

Note that the proposed redistribution mechanism is independent of the specific wavelength on which the registration process is hosted. Consequently, the registration window may be scheduled on any wavelength in any cycle, either fixed to a particular channel or dynamically varied across cycles.

As the system alternates between registration and non-registration cycles, the inter-slot gap experienced by an ONU

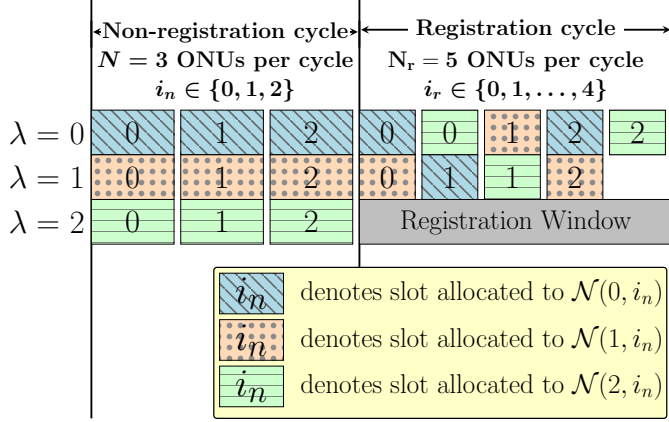


Fig. 6. Example of ONU redistribution for $N = 3$ and $W = 3$. The last slot of wavelength $\lambda = 2$ remains vacant.

during a cycle transition is not uniform across ONUs. Consequently, different ONUs may enter their assigned slot in a given cycle with different residual backlogs, depending on their slot positions relative to the cycle boundary. During each granted transmission opportunity, an ONU attempts to transmit all data buffered in its queue within the allocated slot duration. If the slot duration is sufficient, the buffer is completely drained; otherwise, the remaining backlog is deferred and served in subsequent slots.

The scheduling delay experienced by a frame is therefore jointly determined by the inter-slot gap and the residual backlog carried over from previous cycles. In addition, playout buffers absorb delay variations and reconstruct a uniform output frame stream at the receiver. In the following section, we analytically characterize the per-frame scheduling delay and derive the maximum number of ONUs that can be supported for a given number of wavelength channels.

V. OPTIMIZATION PROBLEM FORMULATION

The primary objective of this formulation is to maximize the total number of supported ONUs NW , or equivalently, to maximize N for a given number of wavelengths W . The formulation begins by defining the slot sizes required to serve the eCPRI traffic. Based on these slot definitions, the evolution of leftover backlog over successive cycles and the resulting worst-case scheduling delays are derived. Finally, the optimization problem implementation and adopted solution methodology are discussed.

Table I lists the system-level parameters and their notation used in the formulation. Other decision variables and derived quantities are defined as they are introduced.

A. Slot sizes

In a TWDM-PON system, each ONU is allocated fixed transmission slots. Under the assumption that all RUs generate traffic at the same eCPRI rate R_C , these slots are identical for all ONUs within a given cycle type. However, to maintain generality, different slot sizes are considered for the two scheduling cycle types, namely registration and non-registration cycles, instead of enforcing a single common slot

TABLE I
DEFINITION OF SYSTEM AND SIMULATION PARAMETERS

Symbol	Description
W	Wavelengths used in each direction
N	ONUs per wavelength in a non-registration cycle
N_r	ONUs per wavelength in a registration cycle (see Eq. (2))
$\mathcal{N}(\lambda, i_n)$	ONU indexed as the i_n on wavelength λ
i_r	Slot index of the ONU $\mathcal{N}(\lambda, i_n)$ in a registration cycle
R_E	Ethernet line rate per wavelength
R_C	Configured eCPRI line rate per ONU
D_b	Scheduling delay budget
T_{reg}	Duration of registration window
T_{gap}	Gap between two registration windows
T_G	Guard band duration
α	Basic eCPRI frame size
E_{max}	Maximum Ethernet payload
L_{hdr}	Ethernet header size

size. The corresponding slot durations are denoted by T_{sr} and T_{sn} , respectively.

These slot sizes are determined by the maximum eCPRI payload (obtained as the product of the maximum number of eCPRI frames and the basic eCPRI frame size) that must be transmitted within a slot, plus the additional overhead introduced by the Ethernet packet headers.

To ensure that a registration-cycle slot can serve *up to* f_r eCPRI frames, the number of Ethernet packets required is

$$p_r = \left\lceil \frac{f_r \alpha}{E_{\text{max}}} \right\rceil, \quad (4)$$

where α is the basic eCPRI frame size and E_{max} is the maximum Ethernet payload size.

Since such a slot must be long enough to transmit $(f_r \alpha + p_r L_{\text{hdr}})$ bits (where L_{hdr} is the Ethernet header size), and must additionally include a guard band of duration T_G at the end of the slot, the registration-cycle slot size T_{sr} must satisfy

$$T_{\text{sr}} \geq \frac{1}{R_E} (f_r \alpha + p_r L_{\text{hdr}}) + T_G. \quad (5)$$

Substituting p_r from (4), the above constraint can be equivalently written as

$$T_{\text{sr}} \geq \frac{1}{R_E} \left(f_r \alpha + \left\lceil \frac{f_r \alpha}{E_{\text{max}}} \right\rceil L_{\text{hdr}} \right) + T_G. \quad (6)$$

Similarly, to serve *up to* f_n frames in a non-registration cycle slot, the corresponding packet count p_n and slot duration T_{sn} satisfy

$$p_n = \left\lceil \frac{f_n \alpha}{E_{\text{max}}} \right\rceil, \quad (7)$$

$$T_{\text{sn}} \geq \frac{1}{R_E} \left(f_n \alpha + \left\lceil \frac{f_n \alpha}{E_{\text{max}}} \right\rceil L_{\text{hdr}} \right) + T_G. \quad (8)$$

Each registration cycle accommodates at most N_r ONUs while each non-registration cycle serves exactly N ONUs. Thus, the durations of the registration and non-registration cycles are

$$T_{\text{cr}} = N_r T_{\text{sr}}, \quad (9a)$$

$$T_{\text{cn}} = N T_{\text{sn}}. \quad (9b)$$

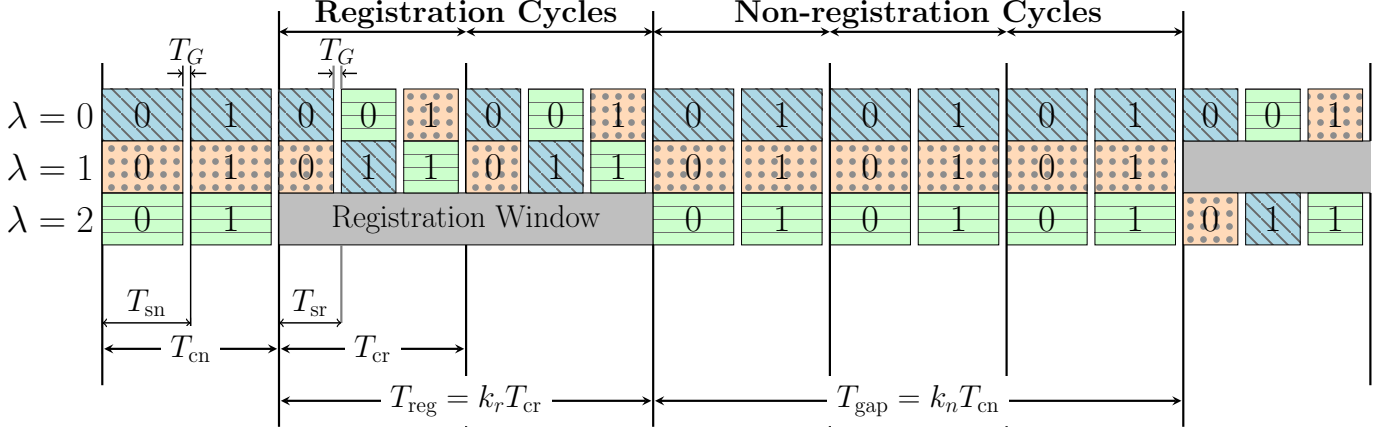


Fig. 7. Scheduling diagram example for $N = 2$, $W = 3$, $N_r = 3$, $k_n = 3$, and $k_r = 2$.

Now, if there are k_r and k_n registration and non-registration cycles respectively, the resulting registration window size T_{reg} and the inter-window gap T_{gap} are

$$T_{\text{reg}} = k_r T_{\text{cr}} = k_r N_r T_{\text{sr}}, \quad (10a)$$

$$T_{\text{gap}} = k_n T_{\text{cn}} = k_n N T_{\text{sn}}. \quad (10b)$$

Figure 7 illustrates these parameters using an example with $N = 2$ and $W = 3$.

B. Delay calculations

This subsection characterizes the worst-case scheduling delay experienced by an ONU over alternating registration and non-registration cycles. The scheduling delay differs across cycles due to variations in the inter-slot gaps; however, the playout buffer at the receiver absorbs these delay variations and enables a time-aligned eCPRI flow toward the DU.

We first define some quantities for use throughout the formulation. For an ONU $\mathcal{N}(\lambda, i_n)$:

- $D_{\text{type}}^{(\lambda, i_n)}[k]$ denotes the maximum scheduling delay experienced by a frame transmitted in the ONU's slot in the k -th cycle of the specified type. In later expressions, we use $D_{\text{reg}}^{(\lambda, i_n)}[k]$ and $D_{\text{nr}}^{(\lambda, i_n)}[k]$ to refer to registration and non-registration cycles, respectively.
- $\Delta_{\text{type}}^{(\lambda, i_n)}[k]$ denotes the time gap between the beginning of the ONU's k -th slot of the specified type and the beginning of its immediately preceding slot.
- $\delta_{\text{type}}^{(\lambda, i_n)}[k]$ denotes the time-equivalent leftover backlog immediately after the ONU's slot in the k -th cycle of the specified type.

The delay analysis follows a simple principle: for any given slot, the maximum scheduling delay of a frame equals the time elapsed since the ONU's previous transmission opportunity plus any backlog remaining at the end of that previous slot. This relationship can be expressed in the generic form

$$D_{\text{type}}^{(\lambda, i_n)}[k] = \Delta_{\text{type}}^{(\lambda, i_n)}[k] + \delta_{\text{type}}^{(\lambda, i_n)}[k - 1]. \quad (11)$$

The leftover backlog evolves across cycles according to

$$\delta_{\text{type}}^{(\lambda, i_n)}[k] = \delta_{\text{type}}^{(\lambda, i_n)}[k - 1] + \Delta_{\text{type}}^{(\lambda, i_n)}[k] - \frac{f_{\text{type}} \alpha}{R_C}, \quad (12)$$

which states that the backlog after the k -th slot equals the backlog remaining after the previous slot, plus the data accumulated during the intervening gap, minus the data transmitted in the current slot. Here, $f_{\text{type}} = f_r$ for registration cycles and $f_{\text{type}} = f_n$ for non-registration cycles.

It is important to note that equations (11) and (12) require special interpretation for the cycle index $k = 0$. In this case, the terms with index $k = -1$ refer to the immediately preceding scheduling cycle, which is the last cycle of the opposite type.

1) Gap between successive slots:

$$\Delta_{\text{reg}}^{(\lambda, i_n)}[0] = (N - i_n) T_{\text{sn}} + i_r T_{\text{sr}}, \quad (13a)$$

$$\Delta_{\text{reg}}^{(\lambda, i_n)}[k] = T_{\text{cr}}, \quad k \in \{1, 2, \dots, k_r - 1\}, \quad (13b)$$

For non-registration cycles

$$\Delta_{\text{nr}}^{(\lambda, i_n)}[0] = i_n T_{\text{sn}} + (N_r - i_r) T_{\text{sr}}, \quad (13c)$$

$$\Delta_{\text{nr}}^{(\lambda, i_n)}[k] = T_{\text{cn}}, \quad k \in \{1, 2, \dots, k_n - 1\}. \quad (13d)$$

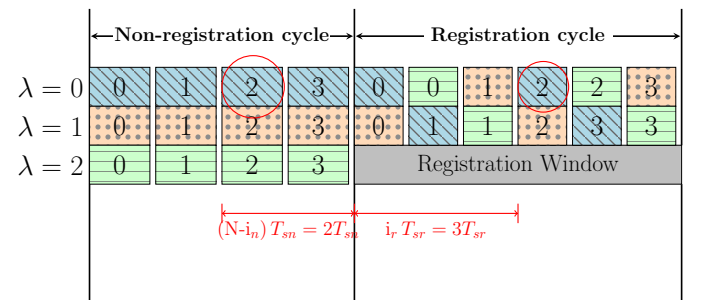


Fig. 8. Illustration of the calculation of the inter-slot gap $\Delta_{\text{reg}}^{(\lambda, i_n)}[0]$ with the example of the ONU $\mathcal{N}(0, 2)$. $\Delta_{\text{nr}}^{(\lambda, i_n)}[0]$ is also calculated similarly.

2) *Leftover data after each slot:* We evaluate the evolution of the leftover backlog in the ONU buffer by traversing the scheduling timeline forward, starting from the transition point where registration cycles begin. The leftover backlog at the end of the last non-registration cycle is zero, since non-registration slots are sized to serve all arriving traffic using the full set of W wavelengths. Consequently, backlog accumulation begins only with the onset of registration cycles.

a) *First registration cycle*: During the gap of duration $\Delta_{\text{reg}}^{(\lambda, i_n)}[0]$, frames arrive at a maximum rate R_C , while at most f_r frames can be transmitted in the subsequent slot. If the accumulated arrivals exceed the slot capacity, a positive backlog remains; otherwise, the backlog is zero. Accordingly,

$$\delta_{\text{reg}}^{(\lambda, i_n)}[0] = \max \left\{ 0, \Delta_{\text{reg}}^{(\lambda, i_n)}[0] - \frac{f_r \alpha}{R_C} \right\}. \quad (14)$$

b) *Subsequent registration cycles*: In a registration cycle, data arrives during the inter-slot gap of duration T_{cr} , while at most f_r frames can be transmitted in the corresponding slot. The difference between these two quantities determines the net backlog accumulated in one registration cycle. So, the leftover evolves linearly as

$$\delta_{\text{reg}}^{(\lambda, i_n)}[k] = \delta_{\text{reg}}^{(\lambda, i_n)}[0] + k \left(T_{\text{cr}} - \frac{f_r \alpha}{R_C} \right), \quad (15)$$

$$\forall k \in \{0, 1, \dots, k_r - 1\}$$

c) *First non-registration cycle*: Using (12), the leftover immediately after the first non-registration slot is

$$\delta_{\text{nr}}^{(\lambda, i_n)}[0] = \delta_{\text{reg}}^{(\lambda, i_n)}[k_r - 1] + \Delta_{\text{nr}}^{(\lambda, i_n)}[0] - \frac{f_n \alpha}{R_C}. \quad (16)$$

d) *Subsequent non-registration cycles*: During the non-registration cycles, the transmission capacity of each slot exceeds the amount of data arriving during the corresponding cycle, resulting in a gradual reduction of the buffered backlog. Accordingly,

$$\delta_{\text{nr}}^{(\lambda, i_n)}[k] = \delta_{\text{nr}}^{(\lambda, i_n)}[0] - k \left(\frac{f_n \alpha}{R_C} - T_{\text{cn}} \right), \quad (17)$$

$$\forall k \in \{0, 1, \dots, k_n - 1\}.$$

To ensure that the excess data accumulated during registration cycles is fully drained within the non-registration phase, we impose the condition

$$\delta_{\text{nr}}^{(\lambda, i_n)}[k_n - 1] \leq 0. \quad (18)$$

This condition implies that the residual backlog becomes zero at or before the $(k_n - 1)$ -th non-registration cycle. Allowing the expression in (18) to take negative values does not affect the worst-case delay analysis and is therefore not explicitly truncated.

3) *Maximum delay*: Using (11), the maximum delay in each cycle follows directly from the corresponding inter-slot gap and the leftover backlog. It is recalled that the terms with index $k = -1$ in (11) and (12) refer to the last scheduling cycle of the opposite type.

For the first registration cycle, no backlog is carried from the preceding non-registration cycle slot, and the delay is therefore equal to the preceding gap alone.

$$D_{\text{reg}}^{(\lambda, i_n)}[0] = \Delta_{\text{reg}}^{(\lambda, i_n)}[0].$$

$$D_{\text{reg}}^{(\lambda, i_n)}[0] = (N - i_n) T_{\text{sn}} + i_r T_{\text{sr}}. \quad (19a)$$

For further registration cycles,

$$D_{\text{reg}}^{(\lambda, i_n)}[k] = \Delta_{\text{reg}}^{(\lambda, i_n)}[k] + \delta_{\text{reg}}^{(\lambda, i_n)}[k - 1].$$

$$D_{\text{reg}}^{(\lambda, i_n)}[k] = T_{\text{cr}} + \delta_{\text{reg}}^{(\lambda, i_n)}[k - 1] \quad (19b)$$

$$\forall k \in \{1, 2, \dots, k_r - 1\}$$

Similarly, for non-registration cycles,

$$D_{\text{nr}}^{(\lambda, i_n)}[k] = \Delta_{\text{nr}}^{(\lambda, i_n)}[k] + \delta_{\text{nr}}^{(\lambda, i_n)}[k - 1].$$

$$D_{\text{nr}}^{(\lambda, i_n)}[0] = i_n T_{\text{sn}} + (N_r - i_r) T_{\text{sr}} + \delta_{\text{reg}}^{(\lambda, i_n)}[k_r - 1]. \quad (20a)$$

$$D_{\text{nr}}^{(\lambda, i_n)}[k] = T_{\text{cn}} + \delta_{\text{nr}}^{(\lambda, i_n)}[k - 1], \quad (20b)$$

$$\forall k \in \{1, 2, \dots, k_n - 1\}$$

4) *Scheduling delay budget constraints*: Let D_b denote the scheduling delay budget. Each ONU must satisfy

$$D_{\text{reg}}^{(\lambda, i_n)}[k] \leq D_b, \quad k \in \{0, 1, \dots, k_r - 1\}, \quad (21a)$$

$$D_{\text{nr}}^{(\lambda, i_n)}[k] \leq D_b, \quad k \in \{0, 1, \dots, k_n - 1\}. \quad (21b)$$

C. Optimization Problem implementation

The optimization problem selects the integer variables f_n , f_r , k_n , and k_r , along with the real-valued slot durations T_{sn} and T_{sr} , to maximize the number of supported ONUs per wavelength N , subject to the slot-allocation constraints in (5) and (8), together with the per-ONU scheduling-delay constraints in (21).

To incorporate the max-operator appearing in the definition of $\delta_{\text{reg}}^{(\lambda, i_n)}[0]$ into the mixed-integer feasibility framework, the expression in (14) is implemented using a standard big- M formulation. Specifically, one binary variable is introduced per ONU to indicate whether the traffic arrivals accumulated during the gap $\Delta_{\text{reg}}^{(\lambda, i_n)}[0]$ exceed the transmission capacity of the corresponding registration-cycle slot. If this condition is satisfied, the leftover backlog is constrained to equal the excess arrivals; otherwise, it is forced to zero.

The ceiling operation in (4) and (7) is implemented by introducing an integer variable for the number of Ethernet packets per slot and enforcing it to lie between the fractional payload requirement and that requirement plus one, thereby ensuring that the variable takes the smallest integer greater than or equal to the corresponding payload-to-packet ratio.

D. Solving the optimization problem

The optimization problem becomes difficult if N , the number of ONUs per wavelength, is treated as a decision variable, since N directly determines the number of ONU-indexed variables and constraints in the formulation. In particular, the binary variables introduced to model the leftover backlog through a big- M construction, as well as the auxiliary variables used to represent the scheduling delay, inter-slot gaps, and leftover backlog, are defined on a per-ONU basis. Allowing N to vary would therefore change the number of decision variables and constraints, resulting in an optimization problem with variable dimension. To address this structural difficulty, a search-based approach is adopted.

We start from the maximum feasible value of N and iteratively decrease N until a valid solution is found that satisfies all system constraints, making each iteration effectively a feasibility problem. The upper limit for the value of N is given by:

$$N_{\text{max}} = \left\lfloor \frac{R_E}{R_C} \right\rfloor, \quad (22)$$

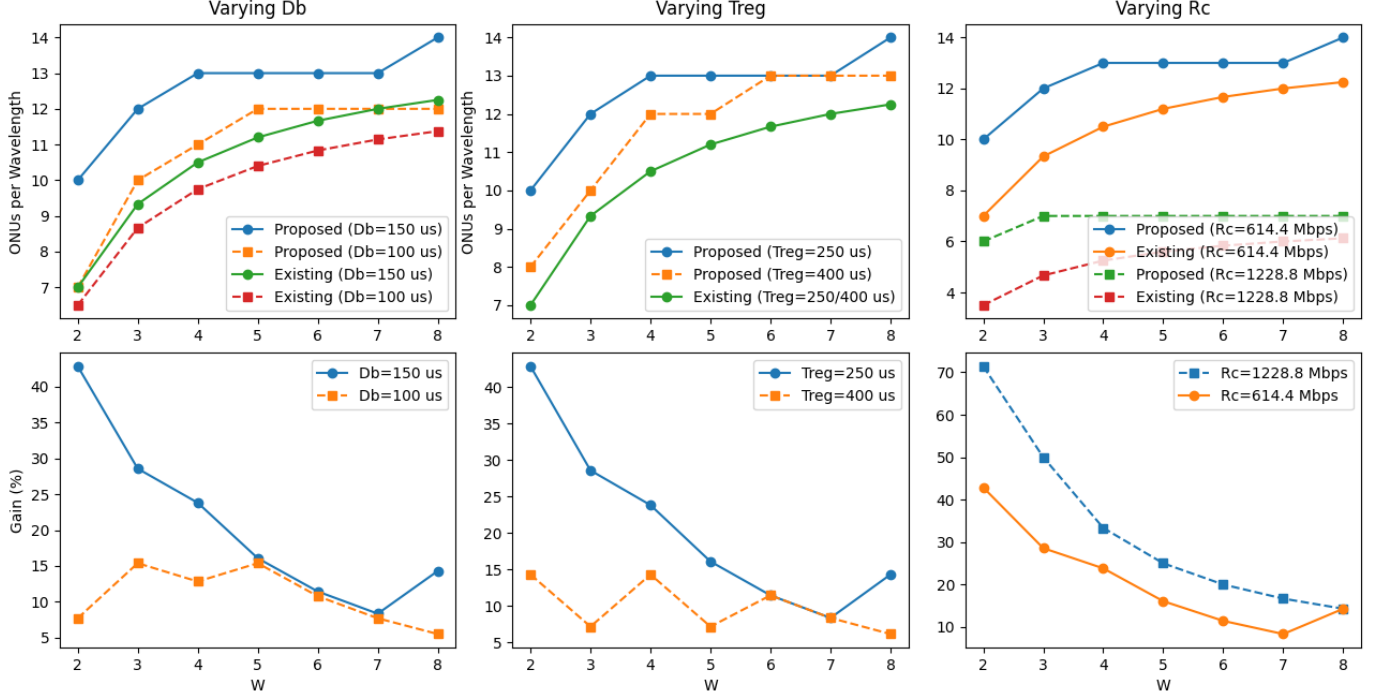


Fig. 9. Percentage gain of the proposed framework versus the number of wavelengths W for different D_b , T_{reg} , and R_C .

In each iteration, N is treated as a constant. The resulting formulation still includes quadratic terms such as $k_n f_n$ and $k_r f_r$, making each iteration a Mixed Integer Quadratic Programming (MIQP) feasibility problem.

Since only a small number of variables are involved and the constraints are tight, a standard solver such as Gurobi [19] can solve each feasibility instance within a fraction of a second. Moreover, since N is fixed per iteration and the problem only checks feasibility, the runtime remains independent of the number of ONUs or wavelengths W . Hence, the system remains computationally tractable and can be solved within milliseconds even for large-scale network scenarios.

VI. RESULTS

In this section, we evaluate the performance of the proposed scheduling framework in terms of the total number of supported RUs for a given number of wavelengths W for three scenarios: (i) varying scheduling delay budgets D_b , (ii) varying registration window sizes T_{reg} , and (iii) varying eCPRI line rates R_C . The results are compared against a baseline approach in which one wavelength is reserved exclusively for registration, as suggested in the ITU-T recommendation [12].

The simulation parameters used, unless stated otherwise, are listed in the following table. The formulated optimization is solved using the Gurobi Optimizer [19].

Fig. 9 shows the percentage gain of the proposed framework as a function of the number of wavelengths W under the considered scenarios, highlighting the performance trends across different delay budgets, registration window durations, and fronthaul rates.

TABLE II
SIMULATION PARAMETERS (UNLESS STATED OTHERWISE)

Symbol	Description	Value
R_E	EPON line rate	10 Gbps
R_C	Configured eCPRI line rate per ONU	614.4 Mbps
D_b	Scheduling Delay Budget	150 μ s
T_{reg}	Duration of registration window	250 μ s
T_{gap}	Gap between two registration windows	100 ms
T_G	Guard band size	1 μ s
α	Basic eCPRI frame size	16 bytes
L_{hdr}	Ethernet header size	26 bytes
E_{max}	Maximum Ethernet payload	1500 bytes

A. Impact of Number of Wavelengths Used

For all configurations, the total number of supported RUs increases with W for both schemes. In the baseline, this increase is strictly linear, since a fixed number of RUs is supported per data-carrying wavelength, with one wavelength exclusively reserved for registration. In contrast, the proposed framework supports a higher and configuration-dependent number of RUs per wavelength by eliminating the need to dedicate a wavelength exclusively to registration.

The relative gain is highest at small W , where reserving one wavelength incurs a substantial effective capacity loss of $1/W$. As W increases, this loss becomes less significant, leading to a gradual reduction in the percentage gain. Nevertheless, the proposed framework maintains a clear advantage across the entire range of W for all configurations.

B. Impact of Delay Budget

As shown in Fig. 9(a) and Fig. 9(d), increasing the scheduling delay budget from $D_b = 100 \mu s$ to $150 \mu s$ consistently improves the achievable gain across all values of W . For the tighter delay budget of $D_b = 100 \mu s$, the gain remains modest, ranging from 5.49% to 15.38%, whereas under the relaxed budget of $D_b = 150 \mu s$ it becomes substantially higher, particularly for small W , reaching up to 42.86% at $W = 2$. This behavior follows from the need to bound the backlog accumulated during registration cycles: tight delay budgets severely restrict the admissible backlog and increase the likelihood of delay violations, while the dedicated-wavelength baseline is largely insensitive to this effect since registration does not introduce additional backlog on data-carrying wavelengths.

C. Impact of Registration Window Size

The impact of the registration window duration is evaluated by comparing $T_{\text{reg}} = 250 \mu s$ and $T_{\text{reg}} = 400 \mu s$ while keeping the scheduling delay budget fixed at $D_b = 150 \mu s$ and the fronthaul rate fixed at $R_C = 614.4 \text{ Mbps}$. As shown in Fig. 9(b) and Fig. 9(e), increasing T_{reg} leads to a gradual reduction in the performance gain of the proposed framework. A larger registration window causes more data to accumulate during each registration cycle, increasing the backlog that must be cleared in subsequent cycles and tightening the delay constraint for a given N and W . Beyond a certain T_{reg} , the delay constraint can no longer be satisfied. In contrast, the dedicated-wavelength baseline remains largely unaffected, since registration is isolated from data-carrying wavelengths. This indicates that the proposed approach is effective only up to a bounded registration window size, which nonetheless covers the range of window durations expected in practical deployments.

D. Impact of eCPRI Line Rate

The effect of the eCPRI line rate is examined using Fig. 9(c) and Fig. 9(f), which respectively show the supported ONUs per wavelength and the corresponding percentage gain as functions of W for different values of R_C , while keeping $T_{\text{reg}} = 250 \mu s$ and $D_b = 150 \mu s$ fixed. It is observed that increasing the eCPRI line rate R_C leads to a higher relative gain of the proposed framework. **Explanation?**

VII. CONCLUSION

We proposed a scheduling framework for a TWDM-EPON-based fronthaul network that supports periodic ONU registration without wasting a dedicated registration wavelength channel, while meeting the stringent delay and jitter constraints imposed by the eCPRI lower-layer splits. Through detailed numerical evaluations, we demonstrated the proposed method achieves up to a 71% increase in the number of RUs supported compared to the existing baseline approach, significantly improving system capacity and resource efficiency.

ACKNOWLEDGMENTS

The authors acknowledge the use of AI-based tools to assist with language editing, clarity, and presentation of the manuscript. All technical content, analysis, and conclusions are verified by the authors.

REFERENCES

- [1] ITU-R Recommendation M.2160-0, "Framework and Overall Objectives of the Future Development of IMT for 2030 and Beyond," ITU-R, Geneva, Switzerland, 2023.
- [2] China Mobile Research Institute, "C-RAN: The Road Towards Green RAN," White Paper, China Mobile, 2011.
- [3] A. Checko, H. L. Christiansen, Y. Yan, L. Scolari, G. Kardaras, M. S. Berger, and L. Dittmann, "Cloud RAN for mobile networks—A technology overview," *IEEE Commun. Surveys Tuts.*, vol. 17, no. 1, pp. 405–426, First Quarter 2015.
- [4] L. Gavrilovska, V. Rakovic, and D. Denkovski, "From cloud ran to open ran," *Wireless Personal Communications*, vol. 113, no. 3, pp. 1523–1539, 2020. [Online]. Available: <https://doi.org/10.1007/s11277-020-07231-3>
- [5] 3GPP, "NG-RAN; Architecture description," 3GPP TS 38.401, V16.3.0, Nov. 2020.
- [6] L. M. P. Larsen, A. Checko, and H. L. Christiansen, "A survey of the functional splits proposed for 5G mobile crosshaul networks," *IEEE Communications Surveys & Tutorials*, vol. 21, no. 1, pp. 146–172, Firstquarter 2019.
- [7] F. Fredrix, "ITU-T Rec. Series G Supplement LLSoT(WDM): Proposed text for Section 7," ITU-T SG15 Contribution 250722-Dxx, Nokia, Teleconference, July 22, 2025.
- [8] A. Fayad, T. Cinkler, and J. Rak, "Toward 6G optical fronthaul: A survey on enabling technologies and research perspectives," *IEEE Communications Surveys & Tutorials*, vol. 27, no. 1, pp. 629–666, Feb. 2025.
- [9] CPRI Cooperation, "Common Public Radio Interface (CPRI) Specification," CPRI V7.0, Oct. 2015.
- [10] eCPRI Consortium, "eCPRI Specification," Version 2.0, May 2020.
- [11] IEEE Standard 802.3av-2009, "Physical Layer Specifications and Management Parameters for 10 Gb/s Passive Optical Networks," IEEE Standard for Ethernet, 2009.
- [12] ITU-T Recommendation G.9804.2 (Amendment 2), "Higher Speed Passive Optical Networks: Physical Media Dependent (PMD) Layer Specification," International Telecommunication Union, Geneva, Aug. 2024.
- [13] L. Liang, W. Lu, M. Tornatore, and Z. Zhu, "Game-assisted distributed decision making to build virtual TDM-PONs in C-RANs adaptively," *Journal of Optical Communications and Networking*, vol. 9, no. 7, pp. 546–554, Jul. 2017.
- [14] A. Mukhopadhyay, D. Korukonda, and G. Das, "Design of Passive Optical Network Based O-RAN X-haul: A Systematic Approach," unpublished, Feb. 2025. [Online]. Available: <https://doi.org/10.36227/techrxiv.174016552.25096358/v1>
- [15] R. Bonk, R. Borkowski, M. Straub, H. Schmuck, and T. Pfeiffer, "Demonstration of ONU activation for in-service TDM-PON allowing uninterrupted low-latency transport links," in *2019 Optical Fiber Communications Conference and Exhibition (OFC)*, 2019, pp. 1–3.
- [16] Y. Zou *et al.*, "DSM-based ultra-low-latency ONU activation for uninterrupted TDM-PON services," *Journal of Lightwave Technology*, vol. 42, no. 1, pp. 128–135, Jan. 2024.
- [17] K. Kim, K. Doo, and H. Chung, "Demonstration of low latency 25G TDM-PON with flexible multizone-based ONU activation for time critical services," in *2022 European Conference on Optical Communication (ECOC)*, 2022, pp. 1–3.
- [18] J. Li, W. Sun, H. Yang, and W. Hu, "Adaptive registration in TWDM-PON with ONU migrations," *Journal of Optical Communications and Networking*, vol. 6, no. 11, pp. 943–951, 2014.
- [19] Gurobi Optimization, LLC, "Gurobi Optimizer Reference Manual," 2025. [Online]. Available: <https://www.gurobi.com>